Basin-scale transport of heat and fluid induced by earthquakes

Chi-Yuen Wang,[1] Lee-Ping Wang,[2] Michael Manga,[1] Chung-Ho Wang,[3] and Chieh-Hung Chen[3]

Received 5 July 2013; accepted 9 July 2013; published 6 August 2013.

[1] Large earthquakes are known to cause widespread changes in groundwater flow, yet their relation to subsurface transport is unknown. Here we report systematic changes in groundwater temperature after the 1999 M_w7.6 Chi-Chi earthquake in central Taiwan, documented by a dense network of monitoring wells over a large (17,000 km^2) alluvial fan near the epicenter. Analysis of the data reveals a hitherto unknown system of earthquake-triggered basin-wide groundwater flow, which scavenges geothermal heat from depths, changing groundwater temperature across the basin. The newly identified earthquake-triggered groundwater flow may have significant implications on postseismic groundwater supply and quality, contaminant transport, underground repository safety, and hydrocarbon production.
Citation: Wang, C.-Y., L.-P. Wang, M. Manga, C.-H. Wang, and C.-H. Chen (2013), Basin-scale transport of heat and fluid induced by earthquakes, *Geophys. Res. Lett.*, *40*, 3893–3897, doi:10.1002/grl.50738.

1. Introduction

[2] Large earthquakes are known to cause widespread changes in groundwater flow at distances thousands of kilometers away from the epicenter [*Brodsky et al*., 2003; *Wang et al*., 2009; *Wang and Manga*, 2010], yet their relation to subsurface transport is poorly understood. Since groundwater flow is effective in transporting subsurface heat [e.g., *Forster and Smith*, 1989; *Ingebritsen et al*., 1989], studies of earthquake-induced changes in groundwater temperature may be useful for better understanding earthquake-induced heat transport. Existing reports on coseismic changes of temperature include that in a hot spring in Japan [*Mogi et al*., 1989], in shallow aquifers in Italy [*Quattrocchi et al*., 2003], in some submarine geothermal systems [e.g., *Sohn et al*., 1998], and near a ruptured fault of a large earthquake in Taiwan [*Wang et al*., 2012]. Analyses in these studies, however, were limited due to lack of regionally distributed data. Here we report systematic change in groundwater temperature across a large (17,000 km^2) alluvial fan (Figure 1). Analysis of the data leads us to identify a hitherto unknown system of earthquake-triggered basin-wide groundwater flow that scavenges geothermal heat from deep beneath the surface, changing groundwater temperature across the basin.

2. Observations

[3] Taiwan is a young mountain belt frequently stricken by large earthquakes. A network of 70 hydrological stations was installed over a large (17,000 km^2) alluvial fan (Figure 1) near the epicenter of the Chi-Chi earthquake. Up to five wells were drilled at each station to depths from tens to 300 m. Well logs show that the alluvial fan consists of several hundred meters of unconsolidated Holocene gravel, sands, and marine mud, with the proportion of gravel to mud increasing from the coast to the upper rim of the fan. Beneath the alluvial fan is a thick (3–5 km) layer of Pliocene-Pleistocene conglomerates laid down in a collisional foreland basin, which, in turn, overlie thick Miocene shales [*Shaw*, 1996; *Lin et al*., 2003].

[4] Groundwater temperature in wells (Figure 1) was measured during routine well maintenance, using an Aqua TROLL200 gauge, manufactured by In-Situ Inc., with accuracy of ±0.1°C. Data were collected 7 months before the earthquake and 2–3 months after the earthquake. The spatial distributions of measured temperature across the basin, both before (Figure 2a) and after (Figure 2b) the earthquake, reveal the nature of earthquake-induced groundwater flow, despite of the lack of temporal continuity. Data from depths less than 100 m are excluded to avoid effects due to surface changes in temperature and recharge.

[5] Groundwater temperatures before the Chi-Chi earthquake are projected onto an east-to-west profile as a function of distance from the surface trace of the ruptured fault in approximately NS direction (Figure 2a). Scatter in the data is partly due to superposition of data from different latitudes onto a single profile. In spite of the scatter, the data show a clear trend of increasing temperature from near the ruptured fault on the east to the coast on the west, indicative of active heat transport by groundwater flow from the upper rim of the alluvial fan across the basin to the coast. Figure 2b shows the groundwater temperature in the same wells 2–3 months after the Chi-Chi earthquake. Here temperatures show the same trend as before the earthquake but is slightly lowered near the ruptured fault and raised near the coast relative to those measured before the earthquake. Figure 2c shows the difference between Figures 2b and 2a, i.e., the *change* in temperature after the earthquake. Despite of the scatter, the data show a clear trend of increase from negative values (temperature decrease) near the eastern rim of the fan near the ruptured fault to positive values (temperature increase) near the coast.

3. Analysis

[6] Three mechanisms were proposed for earthquake-induced change in groundwater systems: static poroelastic

Additional supporting information may be found in the online version of this article.

[1]Earth and Planetary Science, University of California, Berkeley, California, USA.
[2]Department of Chemistry, Stanford University, Stanford, California, USA.
[3]Institute of Earth Sciences, Academia Sinica, Taipei, Taiwan.

Corresponding author: C.-Y. Wang, Earth and Planetary Science, University of California at Berkeley, Berkeley, CA 94720, USA. (chiyuen@berkeley.edu)

0094-8276/13/10.1002/grl.50738

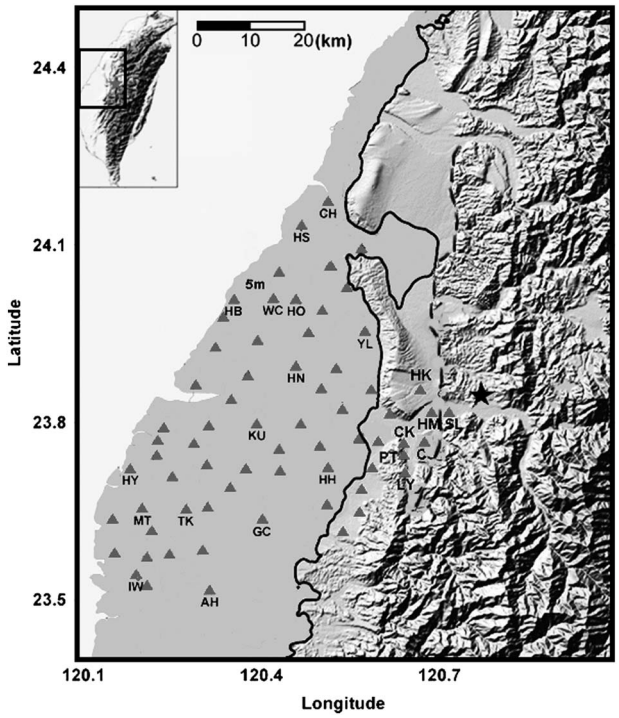

Figure 1. Hydrological stations (triangles) in the study area; those marked with letters have temperature measurements before and after the Chi-Chi earthquake. Star shows the epicenter; dashed curve shows the surface trace of the ruptured fault; black curve shows the thrust front of the Taiwan mountain belt; inset shows the Taiwan island and the location of the study area.

strain [*Wakita*, 1975], shaking-induced consolidation/dilatation of sediments [*Wang et al*., 2001], and enhanced permeability [*Rojstaczer et al*., 1995; *Roeloffs*, 1998; *Brodsky et al*., 2003; *Wang et al*., 2004a]. The first two mechanisms are isotropic and cannot produce the east-to-west trend in the change in groundwater temperature (Figure 2c); the third mechanism could increase the east-to-west groundwater flow and transport under the prevailing downhill head gradient. Here we test this hypothesis by simulating the groundwater flow and transport before and after the earthquake.

[7] We use a two-dimensional, vertical cross section (Figure 3) normal to the ruptured fault. The right boundary of the model coincides with the surface trace of the ruptured fault, and the left boundary lies near the coast. This model is reasonable because the head gradient of groundwater is downhill and normal to the ruptured fault, and the fault is long (>80 km) compared to the width of the alluvial fan (~60 km). The upper 0.5 km of the model represents the Holocene alluvial deposits, and the lower 4 km represents the Plio-Pleistocene conglomerates; the Miocene shale is taken as impervious basement. The model is admittedly highly simplified; however, idealized models have been shown to agree with data and to characterize the first-order hydrological system response to earthquakes [e.g., *Talwani and Acree*, 1985; *Manga*, 2001; *Manga et al*., 2003; *Wang et al*., 2004a; *Manga and Rowland*, 2009; *Wang et al*., 2012].

[8] Groundwater flow is driven by the hydraulic head gradient across the basin. The surface trace of the ruptured Chelungpu fault is at an elevation of ~150 m, yielding an average slope of 0.0025 over the alluvial fan, which is adopted as the head gradient since the water table in central Taiwan is near surface. The average surface temperature near the coast in central Taiwan is about 24°C and decreases eastward at an average rate of 0.02°C/km of horizontal distance across the alluvial fan. The boundary conditions beneath the surface are less certain. For temperature, we assume a vertical heat flux across the lower boundary equal to the measured heat flow of 0.08 W/m^2 from deep exploration wells [*Hwang and Wang*, 1993] and no horizontal heat flux across the two vertical boundaries. For groundwater flow across the eastern vertical boundary, we assume an elevation head equal to that at the surface. This is equivalent to assuming hydrostatic pore pressure beneath the surface on the eastern boundary; it is the most natural assumption near an active fault where rocks are heavily fractured. The hydraulic head across the western vertical boundary may be greater than the hydrostatic head of fresh water due to increased salinity of pore water toward the coast, but the amount of this increase is uncertain.

[9] The flow of groundwater is governed by Darcy's law as follows:

$$\boldsymbol{q} = -\left(\frac{\rho_w g \boldsymbol{k}}{\mu}\right)\cdot\nabla h \tag{1}$$

where $\boldsymbol{q}$ is Darcy's velocity; $\boldsymbol{k}$ is the permeability tensor; ρ_w and μ are the density and the viscosity of pore water, respectively; g is the gravitational acceleration, and h is the hydraulic head. Together with the law of mass conservation, this leads to the following differential equation for groundwater flow (in two dimensions):

$$S_s\frac{\partial h}{\partial t} = \frac{\partial}{\partial x}\left(\frac{\rho_w(T) g k_H}{\mu(T)}\frac{\partial h}{\partial x}\right) + \frac{\partial}{\partial z}\left(\frac{\rho_w(T) g k_V}{\mu(T)}\frac{\partial h}{\partial z}\right) \tag{2}$$

where k_H and k_V are the effective horizontal and vertical permeability, respectively (section 1 of the supporting information); and S_s is the specific storage defined as

$$S_s = \frac{1}{\rho_w(T)}\frac{\partial[n\rho_w(T)]}{\partial h}, \tag{3}$$

where n is the porosity. Hydraulic properties of the alluvial fan before the earthquake are inferred from pump tests and well logs [*Lee and Wu*, 1996; *Tyan et al*., 1996] (section 1 of the supporting information 1). After the earthquake, k_H did not change [*Wang et al*., 2004a], but k_V greatly increased [*Wang et al*., 2004a, 2012]. The hydraulic properties of the conglomerates beneath the alluvial fan are based on recent compilation [*Gleeson et al*., 2011].

[10] Changes in groundwater temperature are obtained by solving the following heat transport equation:

$$\frac{\partial[\rho_b(T)C_b(T)T]}{\partial t} = \nabla\cdot[K_b(T)\nabla T] - \boldsymbol{q}\cdot\nabla[\rho_w(T)C_w(T)T] \tag{4}$$

where C is the specific heat; ρ is the density; K is the thermal conductivity; and subscripts w and b refer to water and bulk sediment properties, respectively. The bulk properties of saturated sediments are approximated as a linear mixture of solid grains and pore water, e.g., $K_b \approx nK_w + (1-n)K_s$, etc., where the subscript s indicates solid grains. Since temperature may affect the density and viscosity of water, which, in turn, may affect the velocity and direction of groundwater flow, we evaluate water properties as functions of

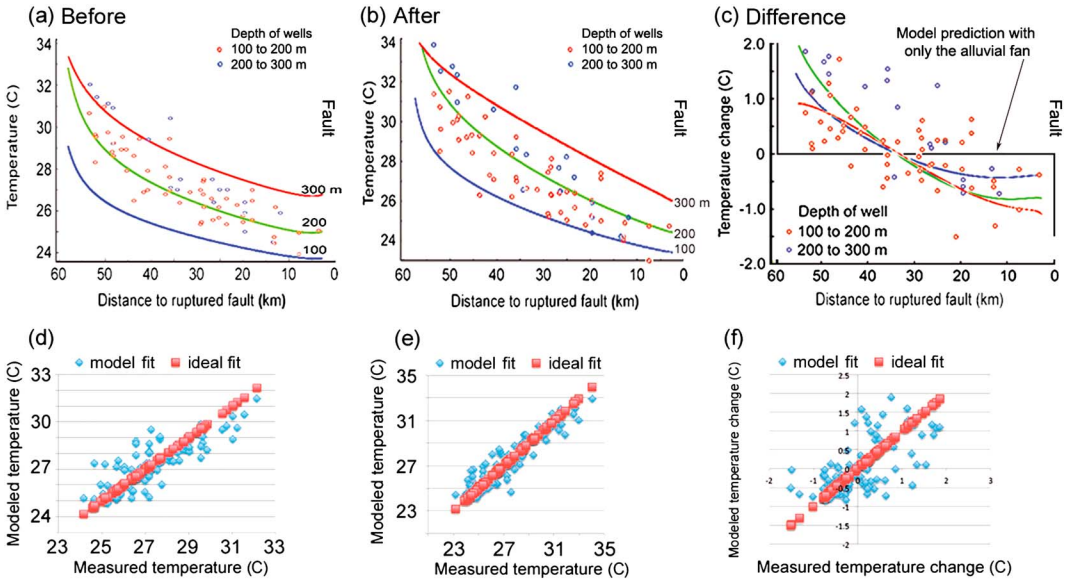

Figure 2. (a) Groundwater temperature in wells on the Choshui alluvial fan ~7 months before the Chi-Chi earthquake. Circles are observed temperatures; different colors show measurements made at depths between 100 and 200 m and between 200 and 300 m, as indicated in the figure. Curves show simulated groundwater temperatures before the earthquake at 100, 200, and 300 m below the surface. Note that numbering on the horizontal axis is from 60 to 0 because distances for data were measured from the fault (right side of figure, as indicated by the word "fault"). (b) Groundwater temperature 2–3 months after the earthquake. Circles are measured temperatures and curves are simulated temperatures 2–3 months after the earthquake. (c) Changes in groundwater temperature after the earthquake (i.e., difference between Figures 2b and 2a). Circles are measured values and curves show simulated values 2–3 months after the earthquake. (d and e) Plots of simulated temperatures against measured temperatures before and after the earthquake, respectively (diamonds). (f): Plot of the difference between simulated temperatures before and after the Chi-Chi earthquake against the difference between measured temperatures before and after the earthquake.

temperature (section 2 of the supporting information) at each time step of the simulation; the effect of pressure is relatively small and neglected.

[11] The system of equations, under described boundary conditions (summarized in Figure 3), is solved numerically using a finite element program (*COMSOL Multiphysics*) and a fine mesh (Figure S1 in the supporting information). The groundwater flow and the temperature before the earthquake are first solved, assuming steady state conditions. These are then used as the initial conditions for calculating the transient changes after the earthquake.

4. Results and Discussion

[12] Figure 2a shows, in colored curves, the simulated groundwater temperature before the Chi-Chi earthquake. The result captures the essential features of the observation, i.e., groundwater temperature increases from the eastern rim of the alluvial fan near the ruptured fault toward the western lowland near the coast. Figure 2d shows the fit to data, with $R^2 = 0.73$.

[13] We next examine if the earthquake-induced change in groundwater temperature could be due to enhanced

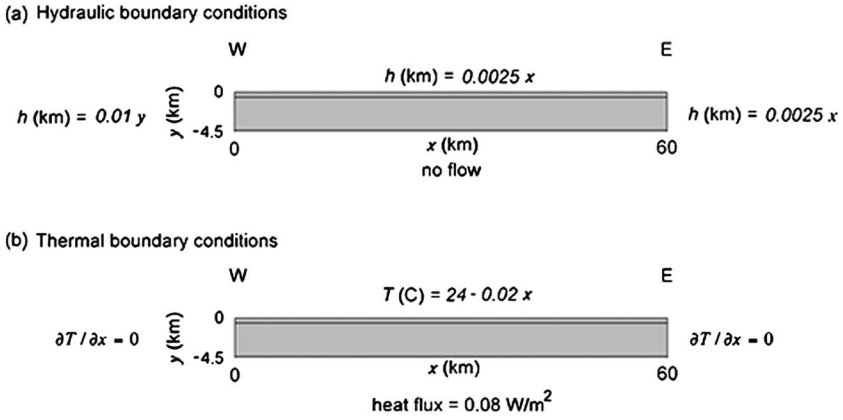

Figure 3. Cross sections showing model geometry and boundary conditions. (a) The hydraulic boundary conditions. (b) The thermal boundary conditions.

Table 1. Hydraulic Properties of Sedimentary Formations Used in Simulation

	Alluvial Fan		Conglomerate	
Geologic Formation	Before	After	Before	After
k_H (m^2)	$10^{-12} f(x)$[a]	$10^{-12} f(x)$	10^{-10}	$10^{-10} + 10^{-8} e^{-t/75\ \text{day}}$
k_V (m^2)	$7.4 \times 10^{-14} f(x)$	$7.4 \times 10^{-14} f(x)(1 + 3 \times 10^3 e^{-t/75\ \text{day}})$	10^{-19}	$10^{-19} + 3 \times 10^{-10} e^{-t/75\ \text{day}}$
Density (kg/m^3)	2600	2600	2600	2600
Porosity	0.3	0.3	0.3	0.3
Thermal conductivity ($W\,m^{-1}\,K^{-1}$)	2.3	2.3	2.3	2.3
Heat capacity ($J\,kg^{-1}\,K^{-1}$)	800	800	800	800
Specific storage (m^{-1})	10^{-6}	10^{-6}	10^{-6}	10^{-6}

[a] $f(x) = 1 + (200x)^{1/3}$: functional form assumed for the spatial distribution of effective permeability to reflect the increased proportion of gravel to mud from the coast to the ruptured fault near the upper rim of the alluvial fan, where x is the distance from the model coast (Figure 3). The functional form was obtained from numerical experiments to fit the temperature profile before the earthquake.

permeability in the alluvial fan alone (Figure 3, top layer), as assumed in *Wang et al*. [2012]. The simulated temperature change (Figure 2c, black curve) shows no change in groundwater temperature across the basin except near its ends, inconsistent with the data that show gradual changes from east to west across the entire basin (Figure 2c). Thus, the shallow aquifer model in *Wang et al*. [2012] may be inadequate to explain the basin-wide change in groundwater temperature.

[14] The above result may be expected since the *enhanced* groundwater flow would be horizontal if it is confined in the shallow aquifer, and since the isotherms are also nearly horizontal, groundwater temperature will not change except near the ends of the aquifer, where recharge and discharge occur. Widespread changes in groundwater temperature, as shown in Figure 2c, suggest that enhanced transport may have occurred at depths across the entire basin. We use parameter sweep, followed by optimization, to search for k_H and k_V (equation (2)), both in the alluvial fan and in the conglomerate formation below to best fit the temperature data. We also consider the recent result that the enhanced permeability may recover with time to the preearthquake value [*Manga et al*., 2012]. Estimates of recovery time range from a few minutes [*Geballe et al*., 2011] to 6 years [*Kitagawa et al*., 2007]. For the present study, we estimate the recovery time with constraints from data for water level and groundwater temperature. At depths below 100 m, the water level 2–3 months after the earthquake is ~1 m above the preseismic level [*Wang et al*., 2004b]. Numerical experiments with this constraint, assuming exponential decay of the enhanced permeability to the preearthquake value and no lateral flow, lead to a lower-bound estimate of ~15 days for the recovery time. At the same time, groundwater temperature was measured twice in a small number of wells [*Wang et al*., 2012], first 2–3 months after the Chi-Chi earthquake and then 6 months after the earthquake, and these temperatures showed no change with time. This observation requires an upper bound of 2–3 months for the recovery time; otherwise, there would have been differences between the two sets of temperature data.

[15] Figure 2b shows, in colored curves, the simulated groundwater temperature 2.5 months after the earthquake for a representative model; Figure 2c shows the simulated *change* in groundwater temperature, i.e., the difference between Figures 2b and 2a. The fits to data are given in Figure 2e for the simulated groundwater temperature and in Figure 2f for the *change* in groundwater temperature, with $R^2 = 0.84$ and 0.39, respectively. While the model could be further improved by increasing its complexity and adding more fitting parameters, it fulfills its essential purpose by qualitatively reproducing the trend between temperature change and providing a simple mechanism for this temperature change.

[16] Table 1 lists the parameters for this model. The magnitude of the earthquake-induced permeability change in the simulation (Table 1) is much greater than that estimated by *Elkhoury et al*. [2006]. One reason for this difference may be due to the fact that here, the studied area is in the near field of the Chi-Chi earthquake, while in *Elkhoury et al*. [2006], the wells are in the far field of the respective earthquakes.

[17] The present result suggests that large earthquakes can enhance basin-wide transport and flow to depths of a few kilometers. Earlier studies [*Rojstaczer et al*., 1995; *Claesson et al*., 2007; *Mohr et al*., 2012; *Wang et al*., 2012] suggest that the earthquake-enhanced groundwater flow may be restricted to shallow aquifers. The reason for this disagreement is not entirely clear, but it may partly lie in the fact that, while the earlier studies relied on data from small areas or single wells, the present study integrates data from a large basin, so that differences in temperature are more easily revealed.

[18] Widespread changes in groundwater temperature were also noted after the 2010 Canterbury earthquake in New Zealand [*Cox et al*., 2012]. Thus, earthquake-induced changes in basin-scale transport, as reported here, may also occur in other seismically active areas. Such changes may have important implications on groundwater supply and quality [*Chen et al*., 2012], contaminant transport, and underground waste repositories [*Carrigan et al*., 1991]. Management plans on these issues are currently based on models for preearthquake conditions, which may be inadequate for the conditions following large earthquakes. Reevaluation of management plans may thus be needed to take such changes into account. Finally, basin-wide changes in subsurface permeability following large earthquakes may change hydrocarbon production [*Beresnev and Johnson*, 1994], and repeated changes may alter pathways of hydrocarbon migration.

[19] **Acknowledgment.** We thank two anonymous reviewers for their helpful comments. Research is partly supported by the National Science Foundation.

[20] The editor thanks two anonymous reviewers for their assistance in evaluating this paper.

References

Beresnev, I. A., and P. A. Johnson (1994), Elastic wave stimulation of oil production: A review of methods and results, *Geophysics*, *59*, 1000–1017.

Brodsky, E. E., E. Roeloffs, D. Woodcock, I. Gall, and M. Manga (2003), A mechanism for sustained groundwater pressure changes induced by distant earthquakes, *J. Geophys. Res.*, *108*, 2390, doi:10.1029/2002JB002321.

Carrigan, C. R., G. C. P. King, G. E. Barr, and N. E. Bixler (1991), Potential for water-table excursions induced by seismic events at Yucca Mountain, Nevada, *Geology*, *19*, 1157–1160.

Chen, J. S., C.-Y. Wang, H. Tan, W. Rao, X. Liu, and X. Sun (2012), New lakes in the Taklamakan Desert, *Geophys. Res. Lett.*, *39*, L22402, doi:10.1029/2012GL053985.

Claesson, L., A. Skelton, C. Graham, and C.-M. Morth (2007), The timescale and mechanisms of fault sealing and water-rock interaction after an earthquake, *Geofluids*, *7*, 427–440.

Cox, S. C., H. J. Rutter, A. Sims, T. W. Horton, M. Manga, T. Ezzy, J. J. Weir, and D. Scott (2012), Hydrological effects of the Darfield (Canterbury) Mw7.1 earthquake, 4 September 2010, New Zealand, *N. Z. J. Geol. Geophys.*, 231–247, doi:10.1080/00288306.2012.680474.

Elkhoury, J. E., E. E. Brodsky, and D. C. Agnew (2006), Seismic waves increase permeability, *Nature*, *441*, doi:10.1038/nature04798.

Forster, C., and L. Smith (1989), The influence of groundwater flow on thermal regimes of mountainous terrain: A model study, *J. Geophys. Res.*, *94*, 9439–9451, doi:10.1029/JB094iB07p09439.

Geballe, Z. M., C.-Y. Wang, and M. Manga (2011), A permeability-change model for water level changes triggered by teleseismic waves, *Geofluids*, *11*, 302–308.

Gleeson, T., L. Smith, N. Moosdorf, J. Hartmann, H. H. Durr, A. H. Manning, L. P. H. van Beek, and A. M. Jellinek (2011), Mapping permeability over the surface of the Earth, *Geophys. Res. Lett.*, *38*, L02401, doi:10.1029/2010GL045565.

Hwang, W. T., and C.-Y. Wang (1993), Sequential thrusting model for mountain building: Constraints from geology and heat flow from Taiwan, *J. Geophys. Res.*, *98*, 9963–9973, doi:10.1029/92JB02861.

Ingebritsen, S. E., D. R. Sherrod, and R. H. Mariner (1989), Heat flow and hydrothermal circulation in the Cascade range, north-central Oregon, *Science*, *243*, 1458–1462, doi:10.1126/science.243.4897.1458.

Kitagawa, Y., K. Fujimori, and N. Koizumi (2007), Temporal change in permeability of the Nojima Fault zone by repeated water injection experiments, *Tectonophysics*, *443*, 183–192.

Lee, C. S., and C. L. Wu (1996), Pumping tests of the Choshuichi alluvial fan [in Chinese], in *Conference on Groundwater and Hydrology of the Choshui River Alluvial Fan, Taipei, Taiwan*, pp. 165–179, Water Resour. Bur.

Lin, A. T., A. B. Watts, and S. P. Hesselbow (2003), Cenozoic stratigraphy and subsidence history of the South China Sea margin in the Taiwan region, *Basin Res.*, *15*, 453–478.

Manga, M. (2001), Origin of postseismic streamflow changes inferred from baseflow recession and magnitude-distance relation, *Geophys. Res. Lett.*, *28*, 2133–2136.

Manga, M., and J. C. Rowland (2009), Response of Alum Rock springs to the October 30, 2007, earthquake and implications for the origin of increased discharge after earthquakes, *Geofluids*, *9*, 237–250.

Manga, M., E. E. Brodsky, and M. Boone (2003), Response of stream flow to multiple earthquakes, *Geophys. Res. Lett.*, *30*, 1214–20, doi:10.1029/2002GL016618.

Manga, M., et al. (2012), Changes in permeability caused by transient stresses: Field observations, experiments, and mechanisms, *Rev. Geophys.*, *50*, RG2004, doi:10.1029/2011RG000382.

Mogi, K., H. Mochizuki, and Y. Kurokawa (1989), Temperature changes in an artesian spring at Usami in the Izu Peninsula (Japan) and their relation to earthquakes, *Tectonophysics*, *159*, 95–108, doi:10.1016/0040-1951(89)90172-8.

Mohr, C. H., D. R. Montgomery, A. Huber, A. Bronstert, and A. Iroumé (2012), Streamflow response in small upland catchments in the Chilean coastal range to the M_w8.8 Maule earthquake on 27 February 2010, *J. Geophys. Res.*, 117, F02032, doi:10.1029/2011JF002138.

Quattrocchi, F., R. Favara, G. Capasso, L. Pizzino, R. Bencini, D. Cinti, G. Galli, F. Grassa, S. Francofonte, and G. Volpicielli (2003), Thermal anomalies and fluid geochemistry framework in occurrence of the 2000–2001 Nizza Monferrato seismic sequence (northern Italy): Episodic changes in the fault zone heat flow or chemical mixing phenomena?, *Nat. Hazards Earth Syst. Sci.*, *3*, 269–277, doi:10.5194/nhess-3-269-2003.

Roeloffs, E. A. (1998), Persistent water level changes in a well near Parkfield, California, due to local and distant earthquakes, *J. Geophys. Res.*, *103*, 869–889.

Rojstaczer, S., S. Wolf, and R. Michel (1995), Permeability enhancement in the shallow crust as a cause of earthquake-induced hydrological changes, *Nature*, *373*, 237–239.

Shaw, C.-L. (1996), Statigraphic correlation and isopach maps of the western Taiwan basin, *TAO*, *7*, 333–360.

Sohn, R. A., D. J. Fornari, K. L. Von Damm, J. A. Hildebrand, and S. C. Webb (1998), Seismic and hydrothermal evidence for a cracking event on the East Pacific Rise crest at 9° 50'N, *Nature*, *396*, 159–161, doi:10.1038/24146.

Talwani, P., and S. Acree (1985), Pore pressure diffusion and the mechanism of reservoir-induced seismicity, *Pure Appl. Geophys.*, *122*, 947–965.

Tyan, C. L., Y. M. Chang, W. K. Lin, and M. K. Tsai (1996), The brief introduction to the groundwater hydrology of Chohui River Alluvial fan [in Chinese], in *Conference on Groundwater and Hydrology of the Choshui River Alluvial Fan, Taiwan*, pp. 207–221, Water Resour. Bur., Taiwan.

Wakita, H. (1975), Water wells as possible indicators of tectonic strain, *Science*, *189*, 553–555.

Wang, C.-Y., and M. Manga (2010), *Earthquakes and Water*, *Lecture Notes in Earth Sci*, vol. *114*, 249 pp., Springer, Berlin.

Wang, C.-Y., L. H. Cheng, C. V. Chin, and S. B. Yu (2001), Coseismic hydrologic response of an alluvial fan to the 1999 Chi-Chi earthquake, Taiwan, *Geology*, *29*, 831–834.

Wang, C.-Y., C. H. Wang, and M. Manga (2004a), Coseismic release of water from mountains: Evidence from the 1999 (*Mw* = 7.5) Chi-Chi earthquake, *Geology*, *32*, 769–772.

Wang, C.-Y., C.-H. Wang, and C.-H. Kuo (2004b), Temporal change in groundwater level following the 1999 (*Mw* = 7.5) Chi-Chi earthquake, Taiwan, *Geofluids*, *4*, 210–220, doi:10.1111/j.1468-8123.2004.00082.x.

Wang, C.-Y., Y. Chia, O.-L. Wang, and D. Dreger (2009), Role of S waves and Love waves in coseismic permeability enhancement, *Geophys. Res. Lett.*, *36*, L09404, doi:10.1029/2009GL037330.

Wang, C.-Y., M. Manga, C.-H. Wang, and C.-H. Chen (2012), Earthquakes and subsurface temperature changes near an active mountain front, *Geology*, *40*, 119–122.